135 GPa, the peridotitic mantle solidus temperature extrapolated from our data set is at 4180 ± 150 K. This value is within the range of proposed temperatures on the core side of the CMB, as calculated from an outer-core adiabat and melting experiments on iron alloys (*26*, *27*) or as constrained by the reverse transition from the $CaIrO_3$-type to the perovskite phase at the base of the D″ layer (*28*). Partial melting in the deepest part of the mantle is therefore highly plausible. This process could therefore explain the presence of ULVZs. The close match between the average geotherm and mantle solidus at the CMB may also explain why ULVZs are not observed as a continuous layer in the deep mantle, with thicknesses of partially molten regions varying dramatically from cold to hot mantle areas.

Our results also provide insights in the way an early magma ocean could have crystallized. Partial melting of mantle material and related fractional crystallization will have important geochemical implications in terms of trace elements. This applies for both the inventory of incompatible elements and the isotopic evolution of the Earth. For instance, the semiquantitative analysis made on the sample recovered from 61 GPa shows a clear enrichment of the ferropericlase in iron, and an ubiquitous iron depletion in Mg-perovskite (table S1), which is in agreement with observations made in earlier studies [(*26*) and references therein]. Partial melts enriched in Ca-perovskite and ferropericlase components are thus expected to be denser than a solid residue of Fe-depleted Mg-perovskite. These liquids could have segregated downward and remained at least partly isolated in the lower mantle if mantle convection was not too vigorous [(*29*) and references therein]. Because Ca-perovskite is the major host mineral for many key trace elements, such as U, Th, and rare earth elements (*30*), these liquids could fractionate and host at present many incompatible elements at the core-mantle boundary, thus offering an explanation for primordial chemical signatures at the base of the mantle.

The estimated thickness of such a partially molten layer varies between 0 to 35 km from the intersection of the modern geotherm shown in Fig. 3 with the solidus of the mantle silicate material obtained in our study; however, this thickness could have been as large as 100 km in the Archean, assuming a secular cooling proceeding at a maximum rate of 100 K per billion years (*31*). These features depend on the estimates of the geotherm in the CMB region, which depends on the core thermal profile and temperature. The extension of such partially molten regions would also vary with lateral variations of the geotherm in the lowermost mantle, with the thickest portions occurring at the base of upwelling plumes and a thin layer elsewhere, which is compatible with seismic observations of ULVZs. Such a partially molten layer can alter several properties of the lowermost mantle that could, as proposed earlier (*5*), control the convection regime of the lowermost mantle and the heat transfer between core and mantle and affect the stability of the thermal boundary layer at the CMB.

References and Notes

1. L. H. Kellogg, B. H. Hager, R. D. van der Hilst, *Science* **283**, 1881 (1999).
2. F. Albarede, R. D. van der Hilst, *Philos. Trans. R. Soc. London. A* **360**, 2569 (2002).
3. A. D. Brandon, R. J. Walker, J. W. Morgan, M. D. Norman, H. M. Prichard, *Science* **280**, 1570 (1998).
4. D. J. Frost *et al.*, *J. Geophys. Res.* **115**, B02202 (2010).
5. Q. Williams, E. J. Garnero, *Science* **273**, 1528 (1996).
6. D. Helmberger, T. Lay, S. Ni, M. Gurnis, *Proc. Natl. Acad. Sci. U.S.A.* **102**, 17257 (2005).
7. E. J. Garnero, A. K. McNamara, *Science* **320**, 626 (2008).
8. T. Lay, E. J. Garnero, Q. Williams, *Phys. Earth Planet. Inter.* **146**, 441 (2004).
9. L. X. Wen, D. V. Helmberger, *J. Geophys. Res. Solid Earth* **103** (B8), 17901 (1998).
10. E. J. Garnero, D. V. Helmberger, *J. Geophys. Res. Solid Earth* **103**, 12495 (1998).
11. S. Rost, E. J. Garnero, Q. Williams, *J. Geophys. Res. Solid Earth* **111** (B09310), 1 (2006).
12. S. Labrosse, J. W. Hernlund, N. Coltice, *Nature* **450**, 866 (2007).
13. M. Boyet, R. W. Carlson, *Science* **309**, 576 (2005).
14. Materials and methods are available as supporting material on *Science* Online.
15. E. Ito, A. Kubo, T. Katsura, M. J. Walter, *Phys. Earth Planet. Inter.* **143–144**, 397 (2004).
16. A. Zerr, A. Diegeler, R. Boehler, *Science* **281**, 243 (1998).
17. L. Hennet *et al.*, *Rev. Sci. Instrum.* **73**, 124 (2002).
18. A. Ricolleau *et al.*, *Geophys. Res. Lett.* **36**, L06302 (2009).
19. A. Dewaele, M. Mezouar, N. Guignot, P. Loubeyre, *Phys. Rev. B* **76**, 144106 (2007).
20. D. J. Frost *et al.*, *Nature* **428**, 409 (2004).
21. R. G. Trønnes, D. J. Frost, *Earth Planet. Sci. Lett.* **197**, 117 (2002).
22. J. Zhang, C. Herzberg, *J. Geophys. Res.* **99**, 17729 (1994).
23. K. G. Holland, T. J. Ahrens, *Science* **275**, 1623 (1997).
24. L. Stixrude, N. de Koker, N. Sun, M. Mookherjee, B. B. Karki, *Earth Planet. Sci. Lett.* **278**, 226 (2009).
25. J. M. Brown, T. S. Shankland, *J. R. Astron. Soc.* **66**, 579 (1981).
26. R. Boehler, *Rev. Geophys.* **38**, 221 (2000).
27. Q. Williams, R. Jeanloz, *J. Geophys. Res.* **95**, 19299 (1990).
28. S. Ono, A. Oganov, *Earth Planet. Sci. Lett.* **236**, 914 (2005).
29. C.-T. Lee *et al.*, *Nature* **463**, 930 (2010).
30. A. Corgne, C. Liebske, B. J. Wood, D. C. Rubie, D. J. Frost, *Geochim. Cosmochim. Acta* **69**, 485 (2005).
31. C. Michaut, C. Jaupart, *Earth Planet. Sci. Lett.* **257**, 83 (2007), and references therein.
32. A. Zerr, R. Boehler, *Science* **262**, 553 (1993).
33. A. Zerr, R. Boehler, *Nature* **371**, 506 (1994).

34. We thank L. Hennet and G. Ona Nguema for experimental assistance. X-ray diffraction plots were made using DATLAB software developed by K. Syassen. A.L.A. acknowledges support from Institut National des Sciences de l'Univers (INSU) program "PNP, theme SEDI-TPS," and A.C. acknowledges support from the European Research Council (ERC) under the European Community's Seventh Framework Programme (FP7/2007-2013)/ERC grant agreement 207467. The Focused Ion Beam (FIB) and Scanning Electron Microscope (SEM) facility of the Institut de Minéralogie et de Physique des Milieux Condensés is supported by Région Ile de France grant SESAME 2006 N°I-07-593/R, INSU-CNRS, Institut de Physique (INP)–CNRS, University Pierre et Marie Curie–Paris 6, and by the French National Research Agency (ANR) grant ANR-07-BLAN-0124-01.

Supporting Online Material

www.sciencemag.org/cgi/content/full/329/5998/1516/DC1
Materials and Methods
Figs. S1 to S5
Table S1
References

18 May 2010; accepted 2 August 2010
10.1126/science.1192448

A Test of the Snowball Theory for the Rate of Evolution of Hybrid Incompatibilities

Daniel R. Matute, Ian A. Butler, David A. Turissini, Jerry A. Coyne

Hybrids between species are often sterile or inviable because the long-diverged genomes of their parents cause developmental problems when they come together in a single individual. According to the Dobzhansky-Muller (DM) model, the number of genes involved in these "intrinsic postzygotic incompatibilities" should increase faster than linearly with the divergence time between species. This straightforward prediction of the DM model has remained contentious owing to a lack of explicit tests. Examining two pairs of *Drosophila* species, we show that the number of genes involved in postzygotic isolation increases at least as fast as the square of the number of substitutions (an index of divergence time) between species. This observation verifies a key prediction of the DM model.

Biological speciation involves the evolution of barriers to gene flow between two populations (*1*, *2*). One of the most effective of those barriers, because it is considered irreversible, is "intrinsic postzygotic isolation," the developmentally based inviability or sterility of species hybrids. Dobzhansky (*1*) and Muller (*3*) proposed a simple two-locus model showing how this form of isolation can result from the accumulation of genes that function normally in a pure-species genome but produce epistatic interactions in hybrids.

The classic version of the Dobzhansky-Muller (DM) model, a population-genetics theory for the evolution of reproductive isolation (*2*), begins with

Department of Ecology and Evolution, The University of Chicago, 1101 East 57th Street, Chicago, IL 60637, USA.

*To whom correspondence should be addressed. E-mail: dmatute@uchicago.edu

two loci in an ancestral species having genotype $A_1A_1B_1B_1$ (the model can be expanded to more than two loci). The ancestral species then splits into two geographically isolated descendant species that eventually evolve genotypes $A_1A_1B_2B_2$ and $A_2A_2B_1B_1$ through natural selection, genetic conflict, or sexual selection—or (less likely) genetic drift—that fixes allele A_1 in one species and B_1 in the other. The DM model posits that postzygotic isolation arises as a collateral effect of this evolutionary divergence. In this case, although species having genotypes $A_1A_1B_2B_2$ and $A_2A_2B_1B_1$ at two loci are fit, in hybrids, where the B_2 and A_2 alleles first encounter each other, they interact abnormally, producing sterility or inviability (*1*–*5*).

Although several studies have identified genes causing hybrid incompatibilities (*4*–*8*), little is known about the evolutionary rate at which these incompatibilities arise (*9*, *10*). Mathematical modeling has shown that the expected number of two-locus DM incompatibilities should increase as fast as the square of the number of substitutions between two species, the "snowball effect" (*11*, *12*). (Three-way interactions should increase as fast as the cube of the number of substitutions between two species, and so on.) This is because DM interactions occur between two or more genes from different species, and if individual gene substitutions accumulate at a constant rate within each species, the number of negative epistatic interactions involving at least one gene from each species should grow at least with the square of time elapsed. Because this prediction requires counting genes causing hybrid incompatibilities in at least two different hybridizations between taxa of known divergence times, it cannot be tested in most groups of plants or animals (*2*, *13*–*15*).

We took advantage of the fact that *Drosophila melanogaster* females (*mel*) produce hybrid females when crossed with *D. simulans* (*sim*) and *D. santomea* (*san*) males (*6*, *16*–*18*) to test the snowball prediction of DM theory. We counted the number of incompatibilities that evolved since the divergence of each pair of species; the two pairs have divergence times differing by roughly 2.4 [*mel-sim*: 5.4 million years ago (Ma) and *mel-san*: 12.8 Ma (*19*)].

If we assume that DM interactions occur between pairs of loci, the snowball hypothesis leads us to expect at least six ($\sim 2.4^2$) times as many incompatibilities between the older than between the younger species pair. We tested this prediction through fine-scale mapping and counting of the gene regions causing inviability in hybrid females (the only sex produced by both the *mel* × *sim* and *mel* × *san* crosses).

We crossed females from *D. melanogaster* stocks containing known genomic deletions, or "deficiencies" [Bloomington *Drosophila* Fly Stock Center (*19*)], maintained as heterozygotes against a balancer (*Bal*) chromosome carrying a dominant homozygous lethal mutation, to *san* and *sim* males. We determined the effect of each hemizygous region (presumably expressing recessive alleles from *san* or *sim*) on the viability of hybrid female offspring from the two interspecific crosses (Fig. 1). If a *D. melanogaster* deficiency uncovered a recessive region of the other species' genome producing hybrid lethality when hemizygous in hybrids with *D. santomea*, this cross would produce *Bal/san* but not *Df/san* hybrid females (or, in hybrids with *D. simulans*, *Bal/sim* but not *Df/sim*) (Fig. 1) (*6*, *16*). We considered "inviability regions" to be those yielding relative viability (i.e., the ratio of hybrid progeny carrying the chromosome deficiency to the total number of offspring from that cross) significantly below 0.5 (χ^2 test; $P < 0.05$). This approach detects epistatic interactions between a recessive allele of *D. santomea* (exposed when hemizygous) and a dominant factor in the *mel* genome. Although it is not clear whether we uncovered genes directly involved in speciation—for their divergence may have occurred after speciation was complete—they do represent an evolutionary accumulation of hybrid incompatibilities and thus constitute a test of the snowball effect.

The *mel/san* crosses tested about 92.0% of the *D. melanogaster* genome (calculated as the proportion of total chromosome bands covered in our deficiency screening); the *mel/sim* crosses tested about 79.4% of *D. melanogaster* genome. Finally, to establish whether the deficiencies had an effect on within-species viability when heterozygous in *D. melanogaster* females, we measured the relative viability of deficiency-carrying females in crosses between *D. melanogaster Df/Bal* (*mel Df/Bal*) females and *D. melanogaster* ArkLa males (a stock founded by females from wild populations collected in Arkansas and Louisiana).

The interspecific deficiency screening in *san/mel* hybrids shows 71 nonoverlapping chromosomal regions containing genes involved in DM incompatibilities (Fig. 2 and table S1). In contrast, in *sim/mel* hybrids, we found just 10 regions involved in DM incompatibilities (Fig. 2 and table S2). None of the deficiencies that caused hybrid lethality showed reduced viability in intraspecific crosses, suggesting that the heterozygous-lethal effects are specific to hybrid backgrounds (table S3).

When possible, we used overlapping deficiencies to further localize inviability genes in each cross. This also ensured that the inviability observed with each lethal deficiency could be reproduced with an independent deficiency in the same chromosome region. Of the 71 regions that caused hybrid inviability in *mel/san* hybrids, 61 had overlapping deficiencies, and for each one of these 61 regions, at least one overlapping deficiency showed hybrid inviability. This shows that hybrid inviability is not an artifact of a stock's genetic background and allowed us to further refine the mapping position of each inviability allele (Fig. 2 and tables S1 and S4).

We used Orr's theoretical framework (*4*) to determine the existence of the snowball effect predicted by the DM model, that is, whether the number of genes causing inviability in these two pairs of crosses increased quadratically (or even faster) with their relative divergence times. Because there is no fossil record for these species, we estimated relative divergence times using a genetic proxy: the average number of synonymous substitutions per gene (*Ks*) between each of the two pairs across the whole genome (*20*). Under the assumption of an approximate molecular clock, *Ks* increases linearly with divergence time, and, unlike phylogeny-based estimates, the *Ks*-based estimates of divergence time need not be transformed with calibrations from fossils and make no assumptions about generation times (*20*).

We estimated *Ks* by counting the number of synonymous substitutions for the *sim-mel* (*Ks sim-mel*) and *san-mel* (*Ks san-mel*) species pairs for every sequenced gene shared by these species. These values were then averaged among genes to find the overall *Ks* (and its standard error, or SEM) for each pair of genomes (*Ks sim-mel* = 0.101, SEM = 4.03×10^{-4}; and *Ks san-mel* =

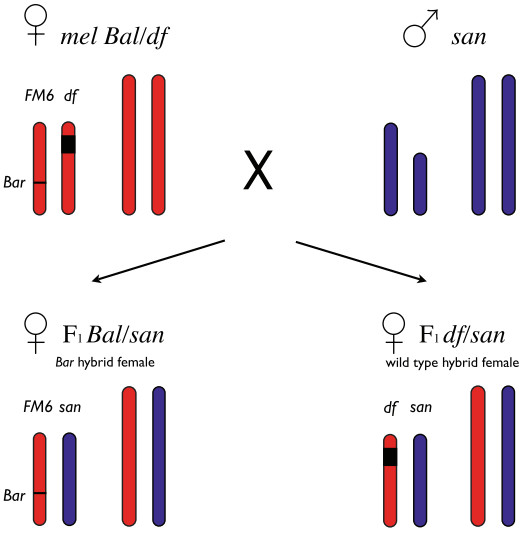

Fig. 1. Crossing scheme used to produce two classes of hybrid female offspring, one of which is hemizygous for a section of *D. santomea* genome uncovered by a deficiency from *D. melanogaster*. This example shows the cross of a *mel* female to a *san* male. If the deficiency does not uncover any lethal allele, half of the progeny will carry the *FM6* balancer paired with a *san* X chromosome; the other half will carry the deficiency paired with a *san* X chromosome. Lethality or semilethality results in a dearth of deficiency-carrying offspring.

0.242, SEM = 8.17×10^{-4}). To establish whether the observed data fulfill theoretical expectations, we calculated the expected number of incompatibilities under two models: one in which incompatibilities accumulated linearly with the number of substitutions (i.e., absence of a snowball effect, which could reflect reproductive isolation caused by nonepistatic factors such as accumulated chromosomal rearrangements), and a model in which the expected number of incompatibilities was proportional to the square of the total number of DNA substitutions (i.e., the presence of a snowball effect involving two-locus interactions). In these calculations we included viability data only for deficiency stocks tested in both sets of crosses (65 incompatibilities in the *mel* × *san* cross and 10 in the *mel* × *sim* cross). To determine which model was more likely to explain the data, we used the AIC [Akaike Information Criterion (*21*)] scores of each model and calculated the evidence ratio of Akaike weights for the quadratic model over the linear model. These scores were then converted to the normalized probability that the quadratic model is preferred over the linear model (*21*).

The *Ks* values, the observed number of incompatibilities, the expected number of incom-

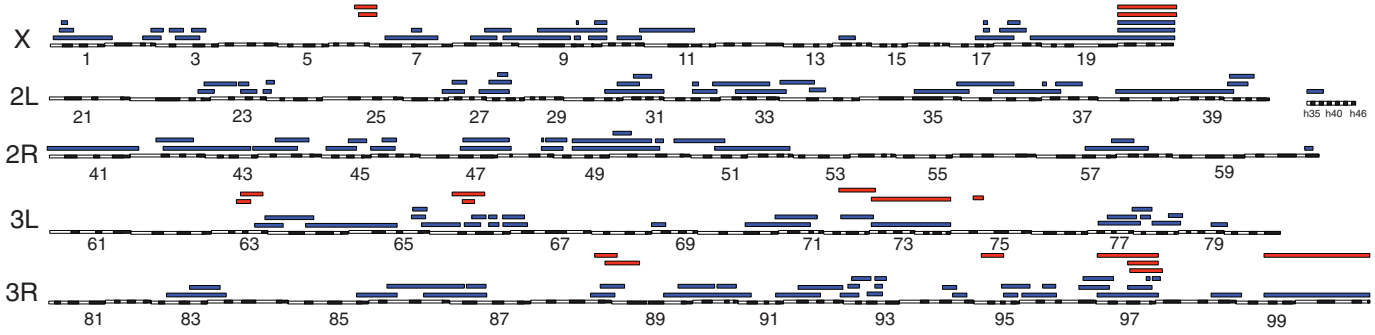

Fig. 2. Chromosomal locations of hybrid lethal regions (on a *D. melanogaster* cytological map) for *D. melanogaster* × *D. santomea* and *D. melanogaster* × *D. simulans* crosses. All lethal regions detected contain at least one gene involved in an epistatic interaction between a recessive element in the *D. santomea* (or *D. simulans*) genome and one or more dominant or semidominant factors in the *D. melanogaster* genome. Regions reducing viability in *mel/san* hybrids are shown in blue; those in *mel/sim* hybrids in red.

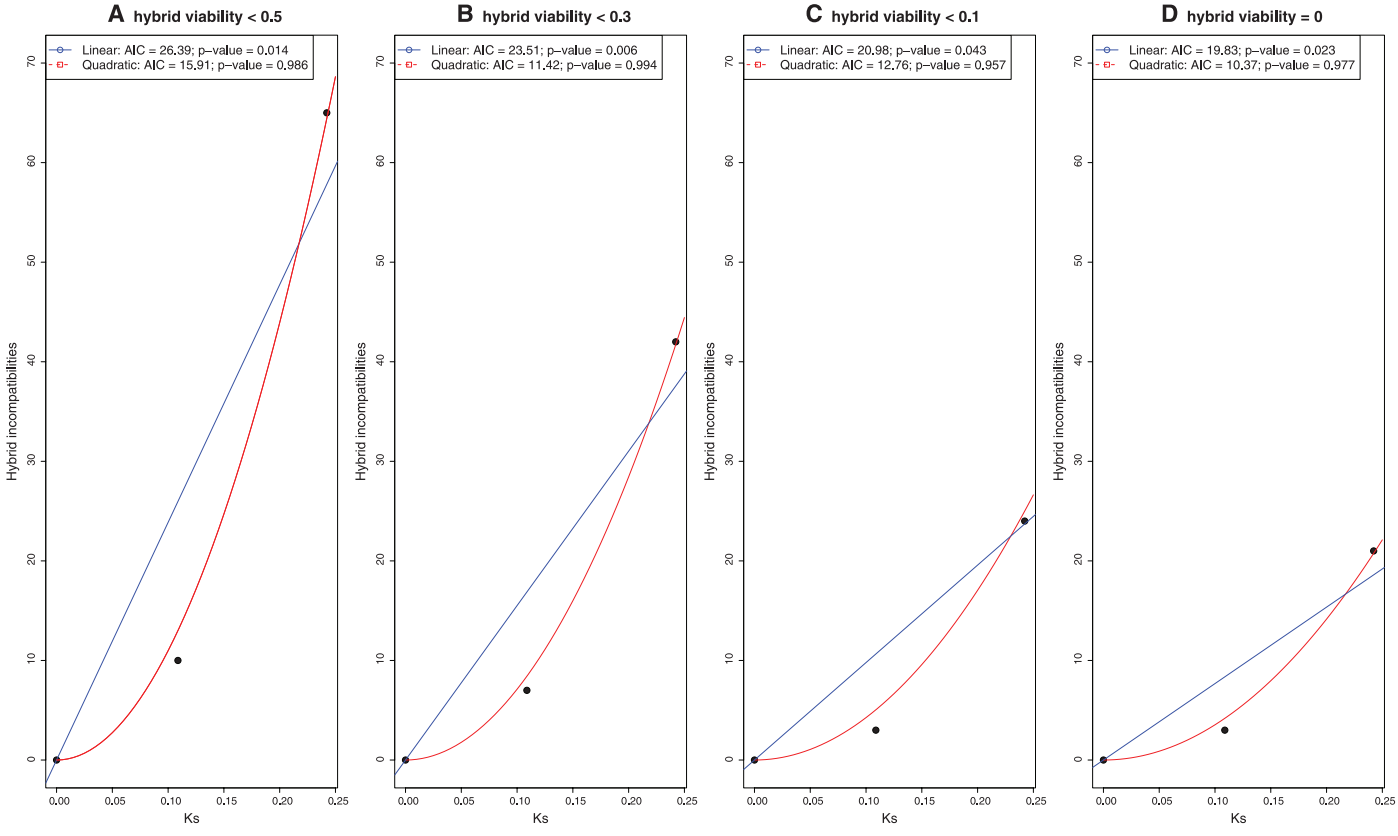

Fig. 3. Number of observed and expected hybrid incompatibilities in *san/mel* and *sim/mel* F_1 female hybrids. We fitted the linear and quadratic model that had lowest AIC values and forced the models through the origin (the assumption here is that at time zero, when there are no genetic substitutions between populations, there are no incompatibilities). *P* values are the normalized probability that each model is to be preferred over the other one (e.g., the quadratic model is to be preferred over the linear model and vice versa) according to the evidence ratio of Akaike weights. Deviations are highly significant for the linear model but not for the quadratic model, regardless of how we quantify "viability"; and in all cases the quadratic model explains the data better than the linear model. Different panels represent the four different definitions of "inviability": (**A**) Lower than 0.5; (**B**) lower than 0.3; (**C**) lower than 0.1; and (**D**) equal to 0.

patibilities, and the results for all the model comparisons are shown in Fig. 3. These data show that the number of incompatibilities does not accumulate linearly with divergence time and is more consistent with a quadratic increase, as expected if the evolution of those incompatibilities obeys the snowball effect. This result holds regardless of which estimate of divergence time we use (Fig. 1 and figs. S1 to S3). We thus conclude that hybrid incompatibilities between these species accumulate substantially faster than linearly with respect to their divergence time.

In addition to fitting the linear and quadratic models to regions that caused a relative viability lower than 0.5, we used more stringent criteria for inviability, fitting the two models to regions that showed relative viabilities lower than 0.3, 0.1, and 0. The results were similar in all cases (Fig. 1 and figs. S1 to S3) and revealed that, regardless of their size, deleterious epistatic interactions accumulate faster than linearly with divergence time.

Besides counting incompatibilities, our results can be used to identify and isolate genes causing reproductive isolation between species. Deletion mapping in *D. melanogaster/D. simulans* hybrids has identified two "hybrid inviability" genes with function in nuclear transport and whose divergence occurred via natural selection (*6*, *8*, *22*).

By confirming a key prediction of the DM theory and showing a snowball effect of the accumulation of genetic incompatibilities causing reproductive isolation, we support the view that postzygotic reproductive isolation often results from deleterious interactions in hybrids between genes that behave normally within species.

References and Notes

1. T. Dobzhansky, *Genetics and the Origin of Species* (Columbia Univ. Press, New York, 1937).
2. J. A. Coyne, H. A. Orr, *Speciation* (Sinauer Associates, Sunderland, MA, 2004).
3. H. J. Muller, *Biol. Symp.* **6**, 71 (1942).
4. D. C. Presgraves, *Curr. Biol.* **17**, R125 (2007).
5. N. Phadnis, H. A. Orr, *Science* **323**, 376 (2009).
6. D. C. Presgraves, *Genetics* **163**, 955 (2003).
7. N. J. Brideau *et al.*, *Science* **314**, 1292 (2006).
8. S. Tang, D. C. Presgraves, *Science* **323**, 779 (2009).
9. S. Gourbière, J. Mallet, *Evolution* **64**, 1 (2010).
10. N. Johnson, in *Evolutionary Genetics: Concepts and Case Studies*, C. W. Fox and J. B. Wolf, Eds. (Oxford Univ. Press, New York, 2006), pp. 374–386.
11. H. A. Orr, *Genetics* **139**, 1805 (1995).
12. H. A. Orr, M. Turelli, *Evolution* **55**, 1085 (2001).
13. L. C. Moyle, T. Nakazato, *Genetics* **179**, 1437 (2008).
14. D. I. Bolnick, T. J. Near, *Evolution* **59**, 1754 (2005).
15. L. C. Moyle, B. A. Payseur, *Trends Ecol. Evol.* **24**, 591 (2009).
16. J. A. Coyne, S. Simeonidis, P. Rooney, *Genetics* **150**, 1091 (1998).
17. D. R. Matute, I. A. Butler, J. A. Coyne, *Cell* **139**, 1180 (2009).
18. Materials and methods are available as supporting materials on *Science* Online.
19. K. Tamura, S. Subramanian, S. Kumar, *Mol. Biol. Evol.* **21**, 36 (2004).
20. W. H. Li, *J. Mol. Evol.* **36**, 96 (1993).
21. K. P. Burnham, D. R. Anderson, *Model Selection and Multimodel Inference: A Practical Information-Theoretic Approach* (Springer, New York, 2002).
22. D. C. Presgraves, L. Balagopalan, S. M. Abmayr, H. A. Orr, *Nature* **423**, 715 (2003).

23. We thank D. C. Presgraves, T. D. Price, R. Unckless, D. Kennedy, M. A. Sprigge, and M. Przeworski for discussions and reading of the manuscript; P. Andolfatto, T. Hu, and K. Thornton for sharing data; and A. Harris and J. Gladstone for technical help. Funded by NIH grant R01GM058260 (J.A.C.).

Supporting Online Material

www.sciencemag.org/cgi/content/full/329/5998/1518/DC1
Materials and Methods
Figs. S1 to S3
Tables S1 to S4
References

8 June 2010; accepted 27 July 2010
10.1126/science.1193440

Hybrid Incompatibility "Snowballs" Between *Solanum* Species

Leonie C. Moyle[1] and Takuya Nakazato[1,2]

Among the reproductive barriers that can isolate species, hybrid sterility is frequently due to dysfunctional interactions between loci that accumulate between differentiating lineages. Theory describing the evolution of these incompatibilities has generated the prediction, still empirically untested, that loci underlying hybrid incompatibility should accumulate faster than linearly with time—the "snowball effect." We evaluated the accumulation of quantitative trait loci (QTL) between species in the plant group *Solanum* and found evidence for a faster-than-linear accumulation of hybrid seed sterility QTL, thus empirically evaluating and confirming this theoretical prediction. In comparison, loci underlying traits unrelated to hybrid sterility show no evidence for an accelerating rate of accumulation between species.

The Dobzhansky-Muller model of hybrid incompatibility [after (*1*, *2*)] proposes that hybrid sterility and inviability are due to negative genetic interactions between two or more loci [commonly called "Dobzhansky-Muller incompatibilities" (DMIs)] that have accumulated substitutions in diverging lineages. When brought together in hybrids, alleles in each divergent lineage interact dysfunctionally, which results in reduced hybrid fitness (*3*). The action of DMIs is supported by empirical observation of the segregation of sterility in recombinant populations, and the molecular genetic description of individual interacting loci underlying hybrid incompatibility phenotypes (*4*, *5*). The Dobzhansky-Muller model (*3*, *6*–*9*) has produced empirically testable predictions including the "snowball effect"—the number of DMIs accumulating between lineages is expected to "snowball" (increase faster than linearly) with increasing time since lineage divergence (*3*, *6*). Formally, because DMIs are due to gene interactions (epistasis), the number of expected DMIs increases with the square of the number of substitutions differentiating two lineages, when DMIs are due to pairwise epistasis; DMIs due to interactions among more than two loci are expected to accumulate even faster (*6*). Previous attempts to detect the snowball effect by measuring the strength of reproductive isolation between lineages, rather than the number of genes involved, have failed to find a greater-than-linear increase in sterility over time (*10*–*12*). However, testing this theoretical prediction requires information on the number of DMIs contributing to specific isolating barriers among multiple closely related species, rather than simply their phenotypic effects on hybrid sterility (*3*, *6*).

To evaluate the expected snowball of DMIs, we used data from three quantitative trait loci (QTL) mapping experiments among species in the plant genus *Solanum* (*13*–*15*). Each QTL experiment used a unique library of hybrid introgression lines [near-isogenic lines (NILs)] in which all or most of the genome of a wild (undomesticated) *Solanum* species (*Solanum pennellii*, *Solanum habrochaites*, or *Solanum lycopersicoides*) was represented as short individual chromosomal regions serially introgressed into the genetic background of domesticated tomato (*Solanum lycopersicum*). These three experiments are comparable in the mean and distribution of heterospecific introgression sizes and the generations of crossing used to create the lines, and they have similar statistical power for detecting pollen and seed sterility QTL (Table 1) (*15*). Each experiment identified the number, genomic location, and phenotypic effect–size of chromosomal regions associated with two separate postzygotic sterility phenotypes (pollen sterility and seed sterility) acting between two species (*15*). In each population, we also analyzed morphological traits unrelated to hybrid sterility (fruit shape and size of fertile seeds) as an internal control. As a proxy for time since lineage splitting, we estimated pairwise species molecular divergence as the number of synonymous substitutions per synonymous site (K_s) at six unlinked loci distributed throughout the genome (*15*).

[1]Department of Biology, Indiana University, Bloomington, IN 47405, USA. [2]University of Memphis, Memphis, TN 38152, USA.

*To whom correspondence should be addressed. E-mail: lmoyle@indiana.edu

A Test of the Snowball Theory for the Rate of Evolution of Hybrid Incompatibilities

Daniel R. Matute *et al.*

Science **329**, 1518 (2010);
DOI: 10.1126/science.1193440